Extended Abstracts of the 2008 International Conference on Solid State Devices and Materials, Tsukuba, 2008, pp. 952-953

E-7-1 (Invited)

Silicon Integrated Nanophotonics: A Platform for On-Chip Optical Interconnects

William M. J. Green*, Solomon Assefa, Joris Van Campenhout,
Young-Hee Kim, Fengnian Xia, and Yurii A. Vlasov

IBM Thomas J. Watson Research Center
1101 Kitchawan Road, Yorktown Heights, NY 10598, USA
*Email: wgreen@us.ibm.com, Website: www.research.ibm.com/photonics

1. Introduction

As multi-core processor architectures continue to evolve as a promising platform for high-performance computing, an additional set of challenges emerges for the global interconnects between cores. In particular, the limited throughput and large power consumption of electrical interconnects become dominant factors limiting the continued scaling of power performance. One promising solution is to replace conventional global interconnects with a CMOS-compatible intra-chip optical network, based on Silicon-On-Insulator (SOI) nanophotonic integrated circuits.

Two of the functions indispensable within any on-chip optical network include the electrical modulation of an optical carrier at the transmitter, and the routing/switching of this signal throughout the entire network. The recent demonstration of an ultra-compact high-speed silicon Mach-Zehnder modulator and a broadband multi-channel optical switch will be reviewed.

2. Ultra-compact silicon Mach-Zehnder modulators

For on-chip optical interconnect applications, a number of active devices are required, for example electrooptically controlled modulators and switches. The majority of electrooptic silicon photonic devices studied to date have employed carrier injection and/or depletion, and the associated free carrier plasma dispersion effects [1-5]. However, in order for these electrooptic devices to be useful for on-chip optical interconnects, a large number of metrics must be simultaneously optimized, including insertion loss, power dissipation, response time, spectral bandwidth, and footprint. While it may be reasonably straightforward to achieve one or two of these, the design space of possible devices which are optimized for meeting all constraints at the same time becomes very small, and therefore presents a significant challenge unique to on-chip optical interconnects.

We have recently demonstrated ultra-compact free carrier dispersion-based silicon Mach-Zehnder modulators (MZMs) using nanophotonic rib waveguides with integrated p+-i-n+ diodes for carrier injection phase shifters [5]. A cross-section of such an electrooptic waveguide phase shifter is shown in Fig. 1(a). The ultra-compact cross-section of nanophotonic rib waveguides simultaneously confines both the injected free carriers and the fundamental TE mode profile to an effective area of approximately 0.12 μm^2. Localization of both photons and free carriers within such a small region produces extremely efficient phase shifter performance, and permits the design of Mach-Zehnder modulators with an ultra-compact footprint as small as 0.001 mm^2 (L_{MZM} = 100 μm) and a $V_\pi \cdot L$ figure of merit as small as 0.36 V-mm. In comparison with recently published silicon Mach-Zehnder modulators [2, 3], the measured $V_\pi \cdot L$ represents a 100x improvement in the modulation efficiency.

High speed data modulation experiments using a pre-emphasized electrical drive signal with approximately 3.5 V peak amplitude were carried out. Figure 1(b) contains an eyeline diagram of the modulated optical signal at the output of a 200 μm long MZM operating at 10 Gb/s. Under these conditions the modulator consumed a RF power of 51 mW, which translates to an energy of 5 pJ/bit. This high speed, low power performance illustrates that with appropriate design, it is possible to simultaneously satisfy many of the aggressive design metrics for on-chip optical interconnects.

a

b

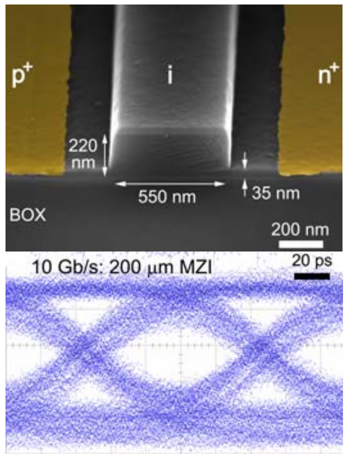

Fig. 1: (a) Cross-sectional SEM image of the SOI p+-i-n+ diode nanophotonic rib waveguide phase shifter used for ultra-compact MZMs. (b) Eyeline diagram of NRZ optical data signal produced by 200 μm long MZM operating at 10 Gb/s.

3. Broadband optical deflection switches

For envisioned on-chip optical network applications where a large aggregate bandwidth is required for communication between cores in a multi-core microprocessor, broadband wavelength-insensitive optical switches are a critical element. As opposed to wavelength-sensitive 2x2 cross-connect switches designed to add or drop messages encoded within individual wavelength channels in telecommunications networks, a wavelength-insensitive switch, also known as a deflection switch [6], should be able to route messages encoded in all available wavelength channels simultaneously, in order to exceed 1 Tb/s aggregate bandwidth between distant microprocessor cores. Additionally, for optical networks monolithically integrated with a silicon multi-core microprocessor, a viable switch device should be capable of accommodating large temperature fluctuations which typically exceed several tens of degrees and occur at variable locations and time intervals depending on processor work load [7]. Owing to the strong thermo-optic effect in silicon, the influence of these dynamical hot spots rules out most of the usual switching approaches based upon high-Q microring resonators [8].

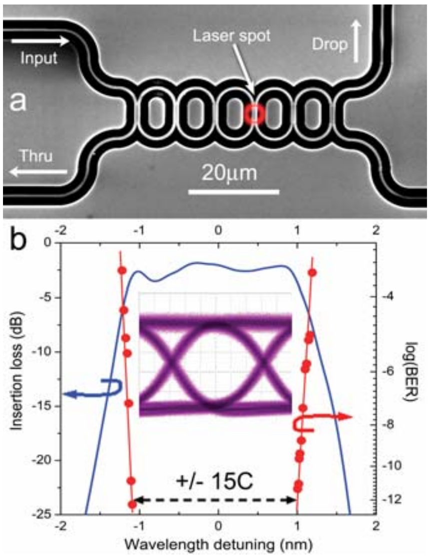

Fig. 2: (a) SEM image of the cascaded microring resonator switch. (b) Transmission spectrum measured at the drop-port (blue curve, left y-axis) superimposed with BER measurements using a 10-Gb/s NRZ signal (red dots, right y-axis).

The device chosen to address these various design aspects is based on an apodized 5th order cascaded silicon microring resonator, as seen in Fig. 2(a) [9]. Appropriate apodization of the coupling coefficients between neighboring high-Q microrings produces a flat-top passband at the drop-port with amplitude ripples less than ±0.5dB. The blue curve in Fig. 2(b) represents a characteristic drop-port transmission spectrum. The 2nm-wide flat-top passband enables the device to transmit optical signals modulated at rates exceeding 100 Gb/s, or alternatively, to accommodate large on-chip temperature variations. This is illustrated by the red dots in Fig. 2(b), which represent the bit error rate (BER) at 10 Gb/s measured at the drop-port while the modulated signal wavelength was scanned across the passband. Error-free (BER<10^{-12}) transmission is observed over the wavelength span exceeding 2nm which closely corresponds to the flat-top passband. The inset shows a typical eye-diagram which stays completely open while the input signal tuned throughout the entire passband. From these measurements, the maximum temperature drift of the passband, illustrated by the black dotted line in Fig. 2(b), can be estimated as 30°C peak-to-peak (±15°C) expected for a realistic on-chip environment [7].

The same device is capable of simultaneously switching a number of parallel data streams from the drop- to the through-port, within adjacent transmission passbands. As illustrated in Fig. 3(a), channels 1 to 9 (1513nm to 1658nm) are all switched at once with a drop-port rejection >15dB, by using a cw Ar-ion pump laser to optically inject free carriers into the central rings, as shown by the laser spot in Fig 2(a). Wavelength-insensitive switching capability is further demonstrated in Fig. 3(b), where a high-speed 40 Gb/s NRZ data signal is injected at the input port using several different wavelength channels, and corresponding waveforms at the thru- and drop-ports are measured for both the ON and OFF states of the switch. The completely open eye-diagrams demonstrate that almost no signal degradation occurs upon switching. Utilizing all the transmission channels shown in Fig. 3(a), an aggregate bandwidth of up to 360 Gb/s may be switched simultaneously. In addition, measurements of the BER at 40 Gb/s have shown that the power penalty for switching is <0.3dB, confirming that this switch design can be useful for realistic optical interconnect applications.

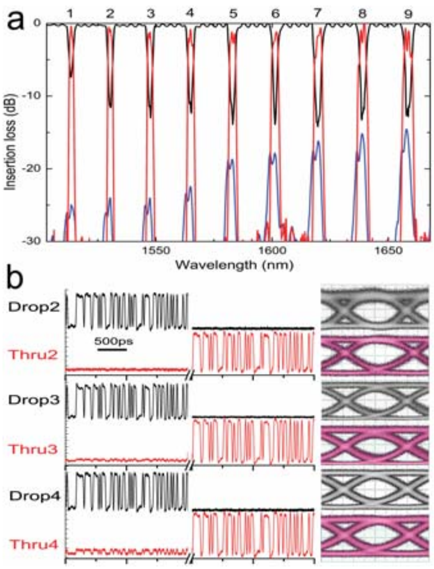

Fig. 3: (a) Drop- (red curve) and thru-port (black curve) transmission spectra of a switch device showing 9 passbands. Blue spectrum depicts drop-port transmission under optical excitation (switch is in ON state). (b) 40 Gb/s multi-channel switch operation.

References

[1] R. A. Soref and B. R. Bennett, IEEE J. Quantum Electron. **23**, 123-129 (1987).
[2] A. Liu, R. Jones, L. Liao, D. Samara-Rubio, D. Rubin, O. Cohen, R. Nicolaescu, and M. Paniccia, Nature **427**, 615-618 (2004).
[3] A. Liu, L. Liao, D. Rubin, H. Nguyen, B. Ciftcioglu, Y. Chetrit, N. Izhaky, and M. Paniccia, Opt. Express **15**, 660-667 (2007).
[4] Q. Xu, B. Schmidt, S. Pradhan, and M. Lipson, Nature **435**, 325-327 (2005).
[5] W. M. J. Green, M. J. Rooks, L. Sekaric, and Y. A. Vlasov, Opt. Express **15**, 17106-17113 (2007).
[6] A. Shacham, K. Bergman, and L. P. Carloni, First International Symposium on Networks-on-Chips, 53-64, Princeton, NJ, 2007.
[7] H. F. Hamann, A. Weger, J. A. Lacey, Z. Hu, P. Bose, E. Cohen, and J. Wakil, IEEE J. Solid-State Circuits **42**, 56-65 (2007).
[8] P. Dong, S. F. Preble, and M. Lipson, Opt. Express **15**, 9600-9605 (2007).
[9] Y. Vlasov, W. M. J. Green, and F. Xia, Nature Photonics **2**, 242-246 (2008).